Eur. Phys. J. D **19**, 57–64 (2002)
DOI: 10.1140/epjd/e20020055

THE EUROPEAN PHYSICAL JOURNAL D
EDP Sciences

Landau fragmentation and deformation effects in dipole response of sodium clusters

V.O. Nesterenko[1,a], W. Kleinig[1,2], and P.-G. Reinhard[3]

[1] Bogoliubov Laboratory of Theoretical Physics, Joint Institute for Nuclear Research, Dubna 141980, Moscow region, Russia
[2] Technische Universität Dresden, Institut für Analysis, 01062 Dresden, Germany
[3] Institut für Theoretische Physik, Universität Erlangen, 91058 Erlangen, Germany

Received 26 October 2001 and Received in final form 11 December 2001

Abstract. Recent experimental data on the dipole plasmon in axial sodium clusters Na_N^+ with $11 \leq N \leq 57$ are analyzed within a self-consistent separable random-phase approximation (SRPA) based on the deformed Konh-Sham functional. Good agreement with the data is achieved. The calculations show that, while in light clusters plasmon properties (gross structure and width) are determined mainly by deformation splitting, in medium clusters with $N > 50$ the Landau fragmentation becomes decisive. Moreover, in medium clusters shape isomers come to play with contributions to the plasmon comparable with the ground state one. As a result, commonly used methods of the experimental analysis of cluster deformation become useless and correct treatment of cluster shape requires microscopic calculations.

PACS. 36.40.-c Atomic and molecular clusters – 36.40.Gk Plasma and collective effects in clusters – 36.40.Vz Optical properties of clusters

1 Introduction

Optical absorption is a key analyzing tool in atomic and molecular systems. It plays a crucial role in the study of clusters since the early days of this field [1]. The prominent feature in the spectra of metal clusters is the surface plasmon resonance (Mie plasmon) [1,2] and accordingly there exists a large body of literature on that topic, see *e.g.* the reviews [3–11]. The plasmon provides valuable information about the underlying cluster geometry which greatly influences cluster properties and is nowadays acquiring relevance for applications [12]. In deformed clusters, the dipole plasmon splits into two (axial shape) or three (triaxial shape) peaks corresponding to dipole oscillations along principle axes of the cluster. The relative heights of the peaks and energy intervals between them provide information on sign and magnitude of the quadrupole moment of the cluster. In practice, the observed photoabsorption cross-section is approximated by one, two or three Lorentzians, and thus the cluster shape is estimated as spherical, axial or triaxial, respectively, see *e.g.* [3]. This feature has been used to establish experimentally a systematics of deformation for Na clusters [13–15]. However, the interpretation in terms of deformation is applicable only if the deformation splitting dominates the gross-structure of the plasmon. On the other hand, we know that Landau fragmentation (the analog of Landau damping for the continues spectrum, defined as fragmentation of the plasmon collective strength over *discrete* particle-hole states due to their coupling to the plasmon) becomes increasingly important with growing cluster size [8,16,17] and the density of isomers does also increase. It is the aim of this paper to investigate theoretically the interplay between deformation splitting, Landau fragmentation and isomeric states in the optical response of Na clusters. To that end, we analyze recent photoabsorption data obtained for cluster ions Na_N^+ with $3 \leq N \leq 64$ [15]. These data cover several size regions of deformed clusters (separated by magic numbers $N = 9, 21, 41$ and 59) and thus allow a systematic study of deformation effects in the optical response.

There exist several approaches for the theoretical description of cluster structure and optical response, ranging from fully fledged quantum-chemical methods for small clusters [18] to a variety of time-dependent local-density-approximation (TDLDA) versions (see the reviews [4,5,8, 11]). TDLDA is a reliable and yet affordable scheme which has been successfully used for the dipole plasmon in clusters since the early calculations of [2]. These first calculations also used a simplified description of the ionic background in terms of a jellium drop. The jellium approximation was often studied since and it turned out to provide a reliable description of Na clusters. To be more precise, the spectra of small Na clusters at very low temperature (*e.g.* 40 K) display fragmentation pattern which can only be explained when using detailed ionic background. These pattern fade away for larger clusters and increasing temperature, which brings the optical response

[a] e-mail: nesteren@theorie2.physik.uni-erlangen.de

close to the one predicted by the jellium model [19]. We thus employ the jellium model for the present study. It may be a bit at the edge for the smallest clusters in our sample but is certainly valid for the larger ones. The optical response explores the regime of small amplitude oscillations. One thus works with the linearized version of TDLDA which is often called random-phase-approximation (RPA). Mind that we mean here an RPA which includes exchange and correlations in the residual interaction. Even though linearized, the RPA grows very elaborate in medium sized deformed clusters. In recent years, we have developed a separable approach to the residual interaction in RPA. It consists of a sum of separable terms which are determined uniquely by the given residual interaction and which can be carried such far that full agreement with the exact RPA results is achieved [16, 17,20,21]. We employ here the separable RPA (SRPA) based on the Kohn-Sham functional for deformed clusters [21]. The method has the advantages (i) to combine the minimal RPA computational effort with high accuracy of the calculations, (ii) to treat on a microscopic level Landau fragmentation, the value which is crucial for the present study.

2 Calculation scheme

The electrons are described by the Kohn-Sham equations using the exchange-correlation functional from [22]. The ionic background is treated within the soft jellium approximation [8] where the ionic density has a form

$$\rho_i(\mathbf{r}) = \frac{\rho_{i0}}{1+\exp((r-R(\Theta))/\alpha)}. \qquad (1)$$

Axial quadrupole and hexadecapole deformations, δ_2 and δ_4, are introduced through the angular dependent cluster radius as

$$R(\Theta) = R_0(1+\sum_{\lambda=2,4}\delta_\lambda Y_{\lambda 0}(\Theta)). \qquad (2)$$

Here $R_0 = Cr_{\rm s}N^{1/3}$; $r_{\rm s} = 3.96$ a.u. is the Wigner-Seitz radius, the coefficient C is adjusted to ensure volume conservation $\int \mathrm{d}\mathbf{r}\rho_i(\mathbf{r}) = N$ and $\rho_{i0} = 3/(4\pi r_{\rm s}^3)$ is the bulk density. The diffuseness of the jellium surface allows to achieve a good reproduction of the empirical plasmon frequency [8,23]. It can be justified by folding of a steep jellium drop with a local ionic pseudo-potential [8]. In our calculations the diffuseness parameter is chosen as $\alpha = 0.8$ which provides the correct global resonance position for the clusters which had been measured at temperature $T = 105$ K [15]. (The larger diffuseness $\alpha = 0.9-1.0$ a.u. as advocated in [8] applies to clusters at room temperature.) The appropriate equilibrium quadrupole (δ_2) and hexadecapole (δ_4) axial deformations are determined by minimization of the energy of the system [21].

Single-electron wave functions of the deformed Kohn-Sham potential are expanded in the complete basis of eigenfunctions of the same but spherical potential and the spherical reference functions are represented on a radial grid in coordinate space. The electronic temperature is handled through thermal occupation weights.

The RPA calculations were performed in the framework of the separable RPA (SRPA) using a systematic expansion and unambiguous determination of the separable terms from the original residual interaction [21]. The separable form dramatically decreases the computational effort, which is highly welcome for deformed clusters where we deal with a huge configuration space. At the same time, SRPA has a numerical accuracy of involved RPA methods [17,21]. SRPA based on the LDA Kohn-Sham functional has been already successfully applied to the description of dipole response in spherical K, Na and Li clusters [17]. In that study the pseudo-Hamiltonian technique was exploited to take into account both local and non-local effects of the ionic structure. The soft jellium approximation [8] used in the present calculations well simulates the local pseudo-potentials which are known to suffice for Na clusters [8,17].

The photoabsorption cross-section for $\mu = 0$ and $\mu = 1$ branches of the dipole response is calculated as

$$\sigma(E1\mu; gr \mapsto j) = \frac{16}{9}\pi^3\frac{\omega_j}{\hbar c}\langle j|rY_{1,\mu}|0\rangle^2 \qquad (3)$$

where $\langle j|rY_{1,\mu}|0\rangle$ is the reduced matrix element of the $E1\mu$ transition from the ground state to the RPA state j.

The results are presented by two ways: (i) as vertical bars for every RPA state to demonstrate the structure of the plasmon and Landau fragmentation, (ii) as the strength function

$$\sigma(E1\mu,\omega) = \sum_j \sigma(E1\mu; gr \mapsto j)\eta(\omega-\omega_j) \qquad (4)$$

smoothed with the Lorentz weight

$$\eta(\omega-\omega_j) = \frac{1}{2\pi}\frac{\Delta}{(\omega-\omega_j)^2+(\Delta/2)^2} \qquad (5)$$

with the averaging parameter $\Delta = 0.25$ eV to simulate a typical broadening of the plasmon (see details in [21]). The latter presentation is convenient for the comparison with experimental data. To simplify the analysis of the gross-structure of the plasmon, we also present the separate contributions to the strength function of $\mu = 0$ and $\mu = 1$ modes of the plasmon.

3 Results and discussion

For our study we have chosen the clusters which, following theoretical estimates [24–30], do exhibit neither triaxiality nor octupole deformation but only even-parity axial deformations. These clusters, Na_{11}^+, Na_{15}^+, Na_{19}^+, Na_{27}^+, Na_{35}^+, Na_{51}^+, Na_{53}^+, Na_{55}^+ and Na_{57}^+ represent three size regions separated by magic numbers $N_{\rm e} = 20$ and 40 ($N_{\rm e}$ is the number of valence electrons). Following *ab initio* calculations [31], Na_{11}^+ has both octupole moment and triaxial contribution. However, since this cluster is widely used as a test for different models, we included it to the list for the completeness.

Table 1. Deformation parameters δ_2 and δ_4 (Eq. (2)) and moments β_2 and β_4 (Eq. (6)), calculated for the ground and isomeric (in Na_{51}^+–Na_{57}^+) states. For isomers the energy deficits ΔE are given.

Cluster	δ_2	δ_4	β_2	β_4	ΔE, eV
Na_{11}^+	0.355	0.25	0.44	0.41	-
Na_{15}^+	0.59	−0.19	0.47	−0.02	-
Na_{19}^+	−0.285	−0.09	−0.21	−0.02	-
Na_{27}^+	0.33	0.08	0.36	0.17	-
Na_{35}^+	−0.21	0.02	−0.18	0.04	-
Na_{51}^+	0.22	0.02	0.23	0.06	-
	−0.16	−0.07	−0.13	−0.04	0.018
Na_{53}^+	0.20	−0.03	0.20	∼0	-
	−0.14	−0.09	−0.11	−0.06	0.016
Na_{55}^+	0.18	−0.07	0.17	−0.05	-
	−0.11	−0.07	−0.09	−0.05	0.020
Na_{57}^+	0.09	−0.03	0.09	−0.02	-
	−0.07	−0.04	−0.06	−0.03	0.004

3.1 Deformation properties

Table 1 collects the deformation parameters and dimensionless moments for the ground and isomeric states of the clusters. Energy deficits of isomers as compared to the ground states are also presented. The δ_λ are the generating deformation as defined in equation (2). The multipole moments β_λ are expectation values of any given distribution and they are defined as

$$\beta_\lambda = \frac{4\pi}{3}\frac{\int \mathrm{d}\mathbf{r}\rho_0(\mathbf{r})r^\lambda Y_{\lambda 0}}{N_\mathrm{e}\tilde{R}}\ , \quad \tilde{R} = \sqrt{\frac{5}{3}\frac{\int \mathrm{d}\mathbf{r}\rho_0(\mathbf{r})r^2}{\int \mathrm{d}\mathbf{r}\rho_0(\mathbf{r})}} \quad (6)$$

where $\lambda = 2, 4$ and $\rho_0(\mathbf{r})$ is ground state density of valence electrons. Unlike the δ_λ which are defined only in connection with the deformed jellium model, the moments β_λ are more general and thus serve for a robust characterization of the deformation and for comparison between different models. The both definitions are tuned to agree for small deformations.

We find that the equilibrium deformation in clusters with $11 \le N \le 35$ is characterized by a deep and distinct minimum of the energy surface. The minimum lies considerably below than for shape isomers. However, increasing cluster size reduces the isomer excitation energy and so enhances the number of relevant isomers. According to this trend, clusters with $51 \le N \le 57$ display a first isomer with a tiny energy deficit, just in reach of the experimental temperature. In contrast to the prolate ground state, the isomer is oblate. Figure 1 shows, as an example, the deformation energy surface of Na_{53}^+ where two distinct minima are seen: the prolate ground state ($\delta_2 = 0.20, \delta_4 = -0.03$) and oblate isomer ($\delta_2 = -0.14, \delta_4 = -0.09$) with the energy deficit of 0.016 eV. Heavier clusters demonstrate more isomers with a small energy deficit [21]. Apparently, such isomers will be present in the thermal ensemble and contribute their part to the observed optical strength.

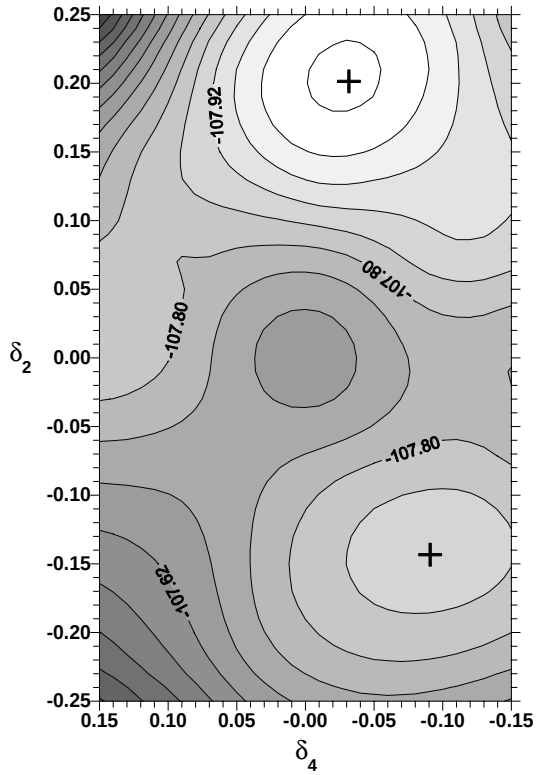

Fig. 1. Energy surface (in eV) of Na_{53}^+ as a function of quadrupole and hexadecapole deformations. The iso-energy counters are separated by intervals 0.06 eV. Two distinct minima are marked by crosses (the energies at the minima are given in Tab. 1).

It worth noting that other jellium studies [27,29,30] also predict prolate ground shape in the size region $51 \le N \le 57$. At the same time, the tiny values of the deficits, obtained in our calculations, point out that the result is fragile and more elaborate schemes can provide another picture. Indeed, pseudopotential calculations [32] predict for these clusters near spherical or slightly oblate shape in the ground state. Such a difference is not significant for aims of the present paper since our main intention is to study a mutual contributions of different shapes to the optical response rather than to determine the true ground state deformations.

3.2 Optical response

The calculated optical response is compared with experimental data [15] in Figures 2 and 3. Figure 2 covers prolate Na_{11}^+, Na_{15}^+, Na_{27}^+ and oblate Na_{19}^+ and Na_{35}^+ clusters. SRPA performs very well in comparison to the data. The main characteristics of the plasmon (energy, deformation splitting, contributions of $\mu = 0$ and $\mu = 1$ modes) are reproduced correctly. It is worth to mention that the calculations use jellium approximation (though soft) which becomes questionable at low temperatures. The temperature $T = 105$ K used in experiment [15] is about at the edge of applicability of jellium approximation, at least for

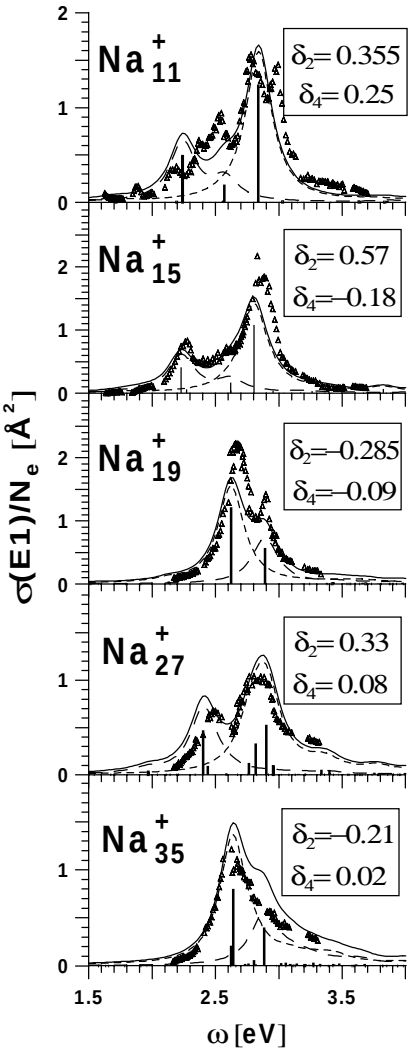

Fig. 2. Photoabsorption cross-section for the dipole plasmon in Na_{11}^+–Na_{35}^+. The deformation parameters are given in boxes. The experimental data [15] (triangles) are compared with SRPA results given as bars for RPA states (3) and as the strength function (4) smoothed by the Lorentz weight. Contributions to the strength function from $\mu = 0$ and 1 dipole modes (the latter has twice larger strength) are given by dashed curves. The bars are given in eV Å^2. See more details in the text.

small clusters. However, our results show that the soft jellium approximation is still good enough even at so low temperature. The main deviations in the description take place for Na_{11}^+ where the experimental data reveal a rich gross-structure of the plasmon. They may be excused by the fact that it is the smallest cluster in our sample. But the difference to well performing Na_{15}^+ is too dramatic. The more likely reason is that Na_{11}^+ goes beyond an axially symmetric approximation. Fully ionic structure optimization shows that it has an octupole moment with strong triaxial contributions [31] (however, even these fully fledged calculations have problems to reproduce the full spectral pattern).

The smaller clusters shown in Figure 2 have a poor Landau fragmentation. In Na_{11}^+, Na_{15}^+ and Na_{19}^+, the $\mu = 0$ and $\mu = 1$ modes are formed, as a rule, by one prominent resonance state. The heavier clusters in Figure 2 show already some Landau fragmentation. But the effect is week and does not modify the gross structure of the response which continues to be determined by the surface plasmon and its deformation splitting. So, in this size region, the gross-structure of the response can be directly used for estimation of the size and magnitude of cluster's quadrupole deformation.

The situation is much more complicated for the spectra of Na_{51}^+–Na_{57}^+ presented in Figure 3. First of all, these clusters demonstrate strong Landau fragmentation, *i.e.* the resonance strength becomes distributed over a bunch of close-by RPA states. The overall shape of the optical strength looks like in smaller oblate clusters, Na_{19}^+ and Na_{35}^+. It has form of a bump with a right shoulder. Just for this reason three of these clusters, Na_{53}^+, Na_{55}^+ and Na_{57}^+, have been interpreted in reference [15] as being oblate. This is in contradiction with our results (see Tab. 1) and other estimates within a jellium approximation [27,29,30], which both predict prolate ground state shapes for these clusters. The middle column of Figure 3 shows the spectra for the oblate isomers. At the first glance, it is surprising: both prolate ground and oblate isomeric states yield optical strength of about the same form. And both strengths reproduce about equally well the experimental data. This puzzle can be solved if we analyze the contributions of $\mu = 0$ and $\mu = 1$ modes to the right shoulder of the plasmon. It is seen that this structure is not the manifestation of $\mu = 0$ mode alone as might be expected (by analogy with clusters Na_{19}^+ and Na_{35}^+) for oblate shape but instead is provided by either $\mu = 1$ mode alone (left plots) or by both $\mu = 0$ and $\mu = 1$ modes together (middle plots). This is in contradiction with a typical picture for oblate systems. At the same time, this result can be easily explained as an effect of Landau fragmentation. It broadens the plasmon resonances so much that the deformation splitting is overruled. Then it becomes clear why the states with so different deformations result nevertheless in a similar plasmon profile. The nature of the right shoulder is discussed in the next section. We will show that this is a shell structure effect specific for a given size region.

Figure 3 allows also to conclude that the plasmon width, evaluated *e.g.*, at its half maximum, is also mainly determined by Landau fragmentation. This should be taken into account while extracting from the complete width their fractions provided by other physical mechanisms (shape fluctuations, interband transitions, etc.).

The right column of Figure 3 shows the strength distribution built as a sum of ground-state and isomer contributions, equally weighted. It leads to a better description than for the ground state or isomer contribution alone. This hints that most probably a mix of prolate ground and oblate isomeric states determines the actual strength. Such conclusion is supported by very low excitation energies of the isomers. One generally assumes that the

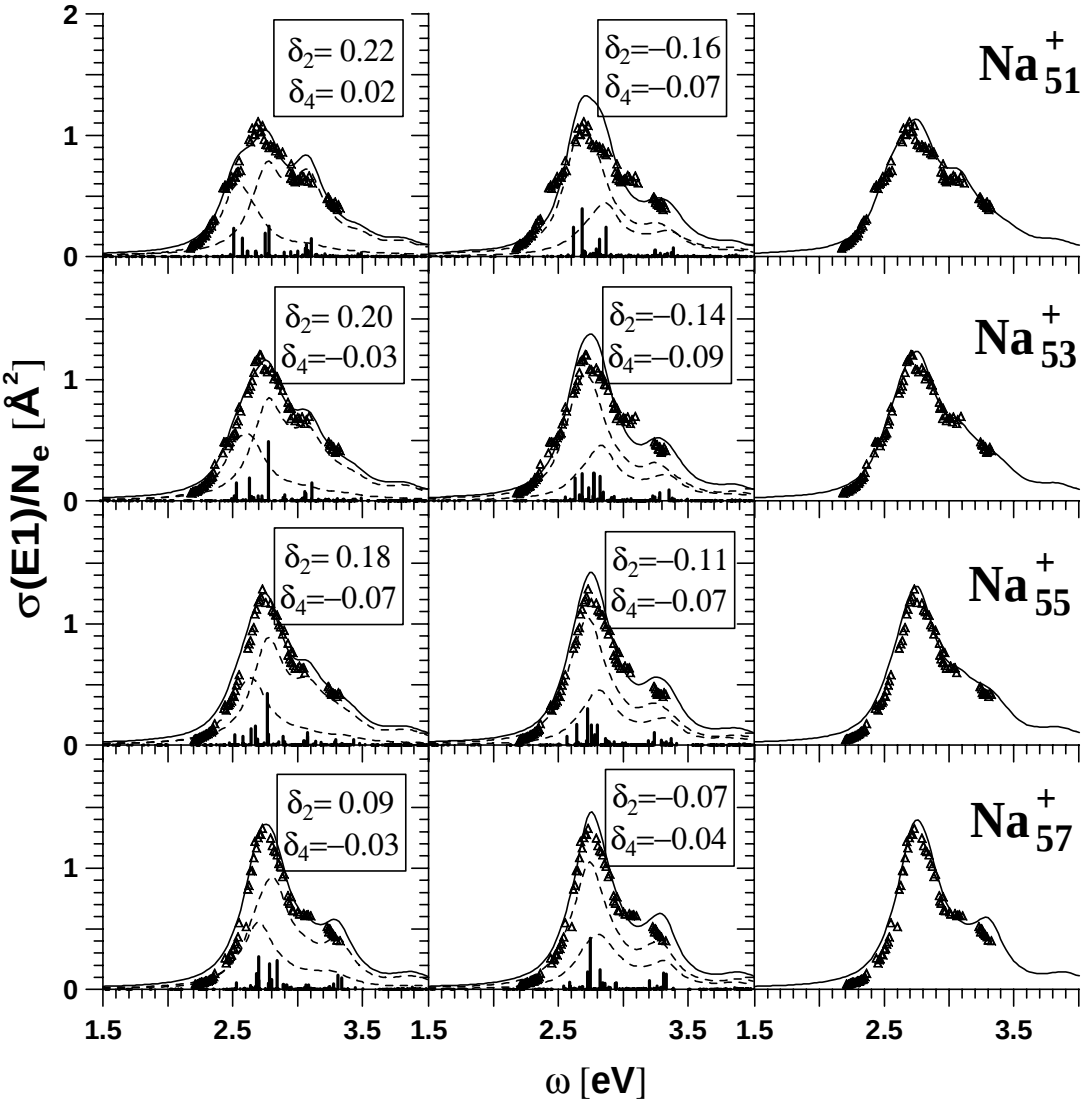

Fig. 3. Photoabsorption cross-section for the dipole plasmon in Na_{51}^+–Na_{57}^+. The experimental data [15] (triangles) are compared with SRPA results for excitations from the prolate ground state (left), oblate isomeric state (middle), both the prolate and oblate states with the half-weighted contributions (right). See Figure 2 for more notations.

thermal ensemble covers a large variety of shapes within energetic reach of the given temperature and that incoherent overlay of the strengths of each shape separately produces a large fraction of the observed plasmon width [33–36]. In fact, the artificial width of 0.25 eV which we use to smooth the spectra serves to account for small thermal fluctuations about each minimum. The mix of the ground state and first isomer is a first step towards a comprehensive isomer mix (which should include also triaxial and parity-breaking shapes) and it seems to work already fairly well for the present examples. The effects discussed here will thus grow in importance when going to larger clusters.

Altogether, the analysis given above shows that in deformed sodium clusters with 50–60 atoms the profile of the plasmon cannot be directly used to deduce the cluster quadrupole deformation. The usual practice to approximate the measured optical response by one, two or three Lorentzians and thus to conclude on spherical, axial or triaxial shape of the cluster becomes dubious. Only microscopic calculations taking into account the interplay of all main physical ingredients can properly treat the gross-structure of optical response and estimate (indirectly) cluster deformation This statement applies for heavier clusters as well. Calculations for deformed clusters with $N > 60$ show that number of isomers with small energy deficit increases with the cluster size [21]. And systematic calculations of the optical response in spherical Na clusters show that Landau fragmentation increases with cluster size, gets a maximum at about $N = 10^3$ atoms and then decreases [16]. The same trend seems to be natural for deformed clusters as well and then our conclusions for Na_{51}^+–Na_{57}^+ can be enlarged for much bigger size region with N up to 10^3. In all these deformed clusters the optical response is predicted as a broad bump with a vague gross-structure where both, gross-structure and width, should be mainly determined by Landau fragmentation. Triaxiality and octupole deformation further entangle the situation. Altogether, this means that in most of deformed clusters, except of small ones with $N < 40$, the measured characteristics of the dipole plasmon cannot be *directly* used for estimation of cluster shape.

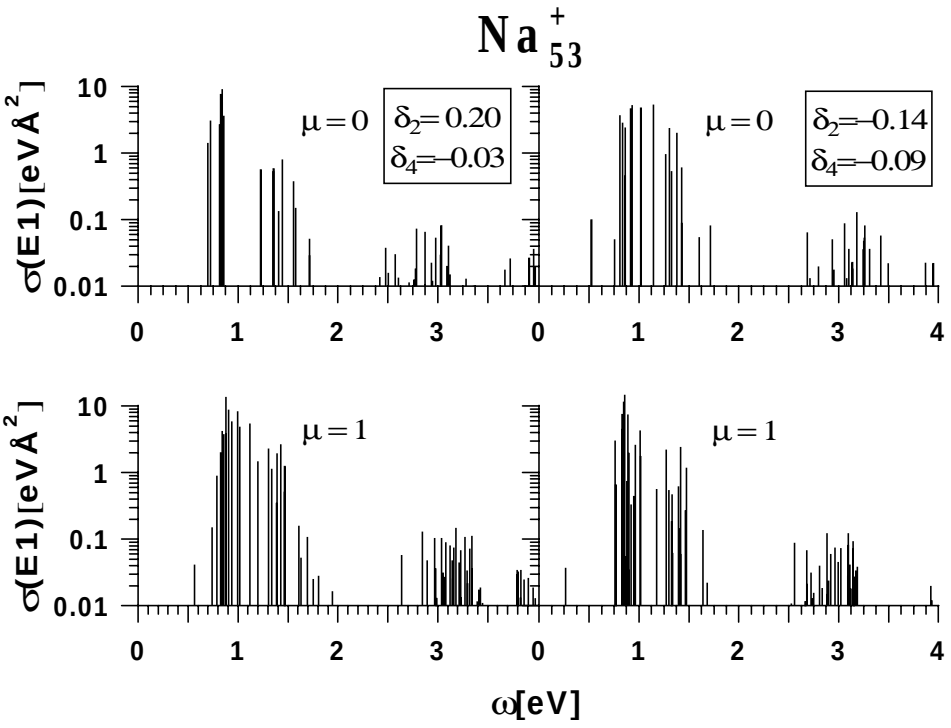

Fig. 4. Unperturbed (without residual interaction) photoabsorption cross-section in Na_{53}^{+} for prolate ground state (left) and oblate isomer (right). Top and bottom plots give contributions of $\mu = 0$ and 1 modes. $\Delta\mathcal{N} = 1$ and 3 bunches are well distinguished at 0.7–1.7 and 2.5–3.5 eV.

Such scenario should be revised for clusters with $N > 10^3$ when Landau fragmentation starts to decrease to extinct finally in the bulk limit. Besides, we gave the arguments for free clusters. Supported clusters demonstrate, at sufficiently big size, oblate shape and distinctive deformation splitting of the dipole plasmon [12].

For clusters in the range just above $N \approx 40$, there is one more chance to extract deformation by adding further empirical data. A promising chance is provided by photo-electron spectroscopy (PES) which gives information on the occupied single electron states. Just recently we have become aware of very systematic and detailed photo-emission spectra for positively charged Na clusters which span a broad range of sizes [37]. A theory-assisted, combined analysis of photo-absorption and PES data can allow to carry the deformation analysis beyond $N \approx 40$.

3.3 The right shoulder in optical response

There had been attempts [30] to explain the right shoulder in the optical response of Na_{51}^{+}–Na_{57}^{+} since the experimental observations of [14]. We will try to sort out the arguments here. The structure cannot be related to the volume plasmon resonance since this mode lies with ∼6 eV at much higher energy. One may think that the right shoulder is caused by the secondary surface plasmon observed at flat metal surfaces, see [38] and references therein. (This mode is also called as the multipole surface plasmon where the term "multipole" reflects nonzero number of poles in the dynamically induced charge density. The Mie plasmon is "monopole" in such terminology.) The mode can be reconstructed in finite clusters by a purely collective electron dynamics. However, it is expected to have little dipole strength and to be heavily fragmented. Thus it is very unlikely that we see a secondary plasmon here.

Last not least, we find that this particular shoulder appears preferably in the range of clusters with $N \simeq 40-90$. This is supported by systematic calculations for singly charged spherical clusters [16,17] which consistently reveal a prominent right shoulder in spectra of K, Na and Li clusters in this size region but not for smaller or heavier clusters (do not confuse a strong right shoulder with a long high-energy tail typical for heavy clusters). This structure is well distinctive in Na and Li clusters and less in K ones. It now happens that the bunch of $1ph$ excitations with $\Delta\mathcal{N} = 3$ ($\mathcal{N}$ is the principle quantum shell number characterizing ordering the shells in cluster mean field) contacts the surface plasmon just in that size range. This is demonstrated in Figure 4 which exhibits the unperturbed (without the residual interaction) dipole strength. The strength is well split into $\Delta\mathcal{N} = 1$ and 3 bunches which correspond to electron transitions from occupied $\mathcal{N}$-shell to unoccupied $(\mathcal{N}+1)$- and $(\mathcal{N}+3)$-shells, respectively. In the size region $N = 50-60$, these bunches are placed at 0.7–1.7 and 2.5–3.5 eV. The bunching takes place for both $\mu = 0$ and 1 modes and for both prolate and oblate shapes. The deformation somewhat spreads the bunching but it remains distinctive. Switching of the shapes, from prolate to oblate, changes mutual positions of the modes but not the picture in general. It is important to note that the center of the $\Delta\mathcal{N} = 3$ bunch lies above the Mie plasmon frequency of 2.7 eV. The plasmon interacts with $\Delta\mathcal{N} = 3$ excitations and donates them a part of the collective strength. The bias of the redistribution of strength is up in energy and this creates the right shoulder.

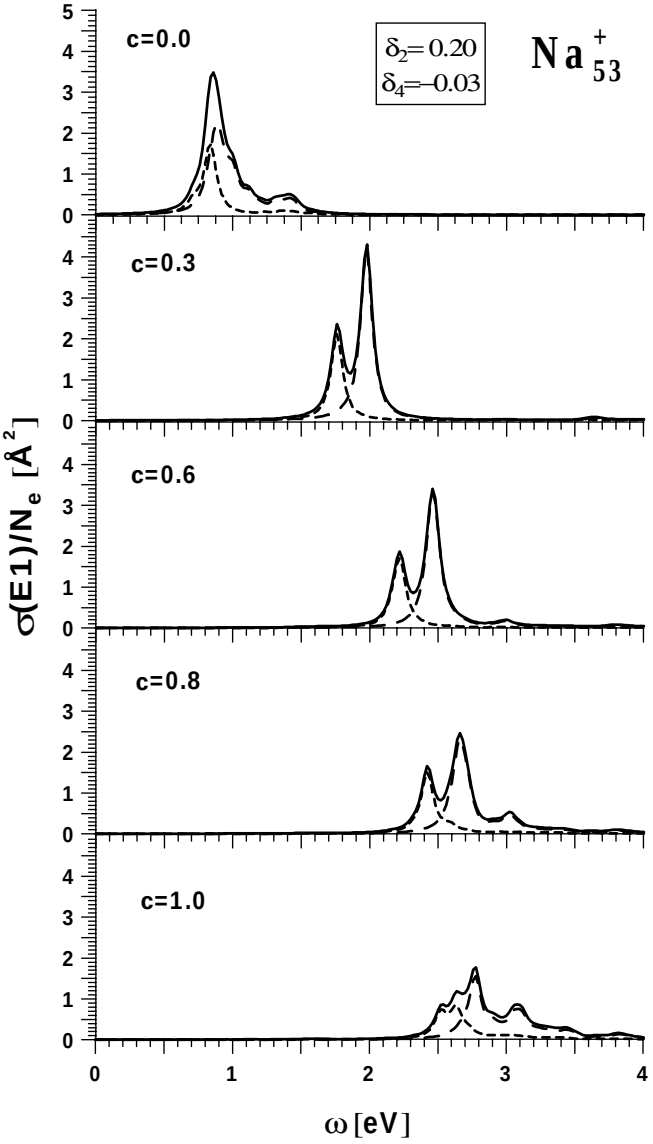

Fig. 5. Photoabsorption cross-section in prolate Na^+_{53}, calculated with residual interaction weighted with the coefficient c. The range from zero ($c = 0.0$) to full scale ($c = 1.0$) interaction is covered. Contributions to the strength function from $\mu = 0$ and 1 dipole modes (the latter has twice larger strength) are given by dashed curves.

The process is illustrated in more detail in Figure 5. The figure shows the optical response with systematically increasing residual interaction, from $c = 0$ (= no residual interaction) to $c = 1$ (= full residual interaction). The photoabsorption strength is drawn with smaller artificial width of $\Delta = 0.15$ eV to make structure effects better visible. It is seen that the Mie plasmon demonstrates a clear two-bump structure as long as it stays far away from $\Delta\mathcal{N} = 3$ excitations (the plots for $c = 0.3{-}0.6$). This is the mere collective splitting. The $\mu = 0$ and 1 modes are well peaked since the plasmon passes an energy region without particle-hole states thus rendering Landau fragmentation negligible. At $c = 0.8{-}1.0$ the plasmon approaches the region with dense $\Delta\mathcal{N} = 3$ spectra but still does not cover it. Strong interaction with $\Delta\mathcal{N} = 3$ states results in two effects: Landau fragmentation of the plasmon at the left flank of $\Delta\mathcal{N} = 3$ spectra and, simultaneously, the pumping some strength to the center of the bunch of $\Delta\mathcal{N} = 3$ states. Such pumping results in the bump at 3.1 eV and, finally, in the right shoulder in the observed optical spectra.

It worth noting that the the right shoulder is not seen in smaller clusters since there the energy interval between $\Delta\mathcal{N} = 1$ and 3 bunches is large and the plasmon does not reach the $\Delta\mathcal{N} = 3$ spectra. *Vise versa*, in heavier clusters the center of the $\Delta\mathcal{N} = 3$ bunch crosses the plasmon peak which removes the bias to higher energies. At the time it comes out below the plasmon frequency, the density of states (including higher bunches with $\Delta\mathcal{N} \geq 5$) is so large that any structures are smoothened or are at most accidental. In that size range one generally sees a long high-frequency tail in the spectra, which is due to the general rule that the density of states increases with increasing energy (see detailed discussion on shell structure effects in optical spectra in [17,39]. Thus we conclude that the right shoulder is a particular case of biased Landau fragmentation applying to a particular size region.

4 Conclusions

A fully self-consistent microscopic approach based on linearized TDLDA (≡ RPA) was applied to the description of recently measured optical response in axially-deformed singly charged sodium clusters with $11 \leq N \leq 57$ [15]. Actually, a separable approach to RPA was used which relies on a systematic and parameter-free expansion thus reproducing full RPA arbitrarily well. Good agreement with the experimental data was achieved. The measurements [15] have been done at rather low temperature, $T = 105$ K. Nevertheless, soft jellium approximation used in our calculations turned out to be accurate enough to provide correct description even for small clusters (with the exception of Na^+_{11}) in our sample.

The calculations show that in light clusters with $N < 40$ the dipole plasmon exhibits a typical two-peak structure reflecting the deformation splitting. Landau fragmentation is here very modest. In the heavier clusters, Na^+_{51}–Na^+_{57}, the dipole spectra have a form of a broad bump with a shoulder on the high-energy side. The shoulder can be explained as a shell structure effect pertinent for this size region. The deformation splitting in these clusters is masked by strong Landau fragmentation which inhibits a direct determination of ground state deformations from the spectra. The calculations predict in Na^+_{51}–Na^+_{57} prolate ground states and oblate shape isomers with very small energy difference. Both prolate ground and oblate isomeric states have surprisingly similar form of the optical strength distribution. This again is due to the large Landau fragmentation which overlays the deformation splitting. Actual experiments deal with a thermal ensemble of isomers. And indeed, a mix of prolate and oblate spectra performs very well in comparison to data.

But, much unlike small clusters, we see here Landau fragmentation as the most important effect for the width and gross structure. We expect a similar scenario for heavier deformed clusters with sizes up to $N \sim 10^3$ atoms. As a consequence, a direct determination of ground state deformation through optical response is inhibited for Na clusters with $N > 40$.

We acknowledge several inspiring discussions with the colleagues B. von Issendorf, H. Haberland, and E. Suraud. The work was partly supported (V.O.N) by RFBR (00-02-17194), Heisenberg-Landau (Germany-BLTP JINR) and DFG (436RUS17/102/01) grants.

References

1. W.A. de Heer, K. Selby, V. Kresin, J. Masui, M. Vollmer, A. Châtelain, W.D. Knight, Phys. Rev. Lett. **59**, 1805 (1987).
2. W. Ekardt, Phys. Rev. Lett. **52**, 1925 (1984).
3. W. De Heer, Rev. Mod. Phys. **65**, 611 (1993).
4. M. Brack, Rev. Mod. Phys. **65**, 677 (1993).
5. G.F. Bertsch, R. Broglia, *Oscillations in finite quantum systems* (Cambridge Univ. Press, 1994).
6. *Clusters of atoms and molecules*, edited by H. Haberland (Springer series in chemical physics, **52**, Springer, Berlin, 1994).
7. C. Bréchignac, J.P. Connerade, J. Phys. B **27**, 3795 (1994).
8. P.-G. Reinhard, O. Genzken, M. Brack, Ann. Physik **5**, 576 (1996).
9. *Metal clusters*, edited by W. Ekardt (Wiley, New-York, 1999).
10. V.O. Nesterenko, W. Kleinig, F.F. de Souza Cruz, in *Proc. of Intern. Workshop "Collective excitations in Fermi and Bose Systems"*, Serra Negra, San Paulo, Brazil, 1998, edited by C.A. Bertulani, L.F. Canto, M.S. Hussein, World Scientific, Singapore, 1999, p. 205; `arXiv:physics/9904017`.
11. F. Calvayrac, P.-G. Reinhard, E. Suraud, C. Ullrich, Phys. Rep. **337**, 493 (2000).
12. T. Wenzel, J. Bosbach, A. Goldman, F. Stietz, F. Träger, Appl. Phys. B **69**, 513 (1999); J. Bosbach, D. Martin, F. Stietz, T. Wenzel, F. Träger, Appl. Phys. Lett. **69**, 2605 (1999).
13. K. Selby, M. Vollmer, J. Masui, V. Kresin, W.A. de Heer, W.D. Knight, Phys. Rev. B **40**, 5417 (1989).
14. P. Meibom, M. Ostergärd, J. Borggreen, S. Bjornholm, H.D. Rasmussen, Z. Phys. D **40**, 258 (1997).
15. H. Haberland, M. Schmidt, Eur. Phys. J. D **6**, 109 (1999).
16. J. Babst, P.-G. Reinhard, Z. Phys. D **42**, 209 (1997).
17. W. Kleinig, V.O. Nesterenko, P.-G. Reinhard, Ll. Serra, Eur. Phys. J. D **4**, 343 (1998).
18. V. Bonačić-Koutecký, P. Fantucci, J. Koutecký, Chem. Rev. **91**, 1035 (1991).
19. H. Haberland, in *Metal clusters*, edited by W. Ekardt (Wiley, New-York, 1999), p. 181.
20. V.O. Nesterenko, W. Kleinig, V.V. Gudkov, N. Lo Iuduce, J. Kvasil, Phys. Rev. A **56**, 607 (1997).
21. W. Kleinig, V.O. Nesterenko, P.-G. Reinhard, Ann. Phys. (N.Y.) (to appear, 2002); `arXiv:physics/0110057`.
22. O. Gunnarson, B.I. Lundqvist, Phys. Rev. B **13**, 4274 (1976).
23. A. Rubio, L.C. Balbas, J.A. Alonso, Z. Phys. D **19**, 93 (1991).
24. B. Montag, P.-G. Reinhard, Z. Phys. D **33**, 265 (1995).
25. S.M. Reimann, S. Frauendorf, M. Brack, Z. Phys. D **34**, 125 (1995).
26. M. Koskinen, P.O. Lipas, M. Manninen, Z. Phys. D **35**, 285 (1995).
27. C. Yannouleas, U. Landman, Phys. Rev. B **51**, 1902 (1995).
28. S. Frauendorf, V.V. Pashkevich, Ann. Physik **5**, 34 (1996).
29. Th. Hirschmann, B. Montag, J. Meyer, Z. Phys. D **37**, 63 (1996).
30. Th. Hirschmann, M. Brack, P.-G. Reinhard, Z. Phys. D **40**, 254 (1997).
31. V. Bonačić-Koutecký, J. Pittner, D. Reichardt, P. Fantucci, J. Koutecký, Czech. J. Phys. **48**, 637 (1998).
32. S. Kümmel, M. Brack, P.-G. Reinhard, Phys. Rev. B **62**, 7602 (2000).
33. C. Yannouleas, R.A. Broglia, Ann. Phys. (N.Y.) **217**, 105 (1992).
34. F. Alasia, R.A. Broglia, H.E. Roman, Ll. Serra, G. Colo, J.M. Pacheco, J. Phys. B **27**, L643 (1994).
35. B. Montag, P.-G. Reinhard, Phys. Rev. B **51**, 14686 (1995).
36. M. Moseler, H. Häkkinen, U. Landmann, Phys. Rev. Lett. **87**, 053401 (2001).
37. G. Wrigge, M. Astruc Hoffmann, B. von Issendorff, preprint 2001.
38. A. Liebsch, Phys. Rev. B **48**, 11317 (1993); A. Liebsch, *Electronic Excitations at Metal Surfaces* (Ser. Physics of Solids and Liquids, Plenum Press, New York and London, 1997).
39. C. Yannouleas, R.A. Broglia, Phys. Rev. B **47**, 9849 (1993).